Investigation of power dissipation in a collimated energy beam

Nan Yu[1, *], Renaud Jourdain[1], Mustapha Gourma[2] and Paul Shore[1, 3]

[1]Precision Engineering Institute, SATM, Cranfield University, MK43 0AL, Bedfordshire, UK

[2]Department of Engineering Computing, SATM, Cranfield University, MK43 0AL, Bedfordshire, UK

[3]Loxham Precision Ltd, Building 90, Cranfield, MK43 0AL, Bedfordshire, UK

**corresponding author (email: n.yu@cranfield.ac.uk;)*

ABSTRACT:

To satisfy the worldwide demand for large ultra-precision optical surfaces, a fast process chain - grinding, polishing and plasma figuring- has been established by the Precision Engineering Institute at Cranfield University. The focus of Cranfield Plasma Figuring team is the creation of next generation of highly collimated energy beam for plasma figuring. Currently, plasma figuring has the capability to shorten processing duration for the correction of metre-scale optical surfaces. High form accuracy can be achieved (e.g. 2.5 hours and 31 nm RMS for 400mm diameter surface). However, it is known that Mid Spatial Frequency (MSF) surface errors are induced when the plasma figuring process is carried out. The work discussed in this paper deals with the characterisation of highly collimated plasma jets delivered by the Inductively Coupled Plasma (ICP) torches. Also a computational fluid dynamics (CFD) model is introduced. This model is used to assess the behaviour of the plasma jet within the best known processing condition. Finally temperature measurement experiments were performed to determine the energy dissipated values that characterise best the ICP torch coil and its De-Laval nozzle.

Keywords: plasma jet, De-Laval nozzle, energy beam, surface processing, material removal footprint

1 Introduction

A variety of scientific and industrial projects, such as segmented ground based telescopes, compact space based observers, short wavelength nano-lithography and high power laser fusion systems, demand metre scale ultra-precise surfaces [1]. Cranfield University and Loxham Precision have been engaged in developing cost-effective fabrication processes for medium to large optical surfaces for the aforementioned applications. A process chain of three sequential machining steps has been proposed. These steps are ultra-precision grinding, robot polishing, and plasma figuring. The fabrication target is to reach a 20 hours cycle time for each stage of surface generation for 1.5m size optics: equating to $1ft^2$ per hour [2].

The final step of this fabrication chain is a state-of-the-art plasma figuring process. This figuring process is a dwell time based and it makes use of an Inductively Coupled Plasma (ICP) torch. The torch displacement is secured by a FANUC CNC motion system. A dedicated dwell time algorithm enables to deliver a controlled chemical reaction for etching local regions of a surface. The use of an ICP torch for the correction of surface aberrations was carried by Carr et al [3] in the late 1990s. Carr's work led to the creation of a series of plasma processing systems. The largest and most advanced plasma figuring machine - called Helios 1200- was delivered and switched on in 2008 at Cranfield. This system was the result of successful collaboration between RAPT Industries and the research team of the Precision Engineering Institute. Helios 1200 is a unique 1.2 metre scale plasma figuring facility housed into the temperature controlled Loxham laboratory [4]. In 2012, Castelli et al [5] demonstrated fast figure correction capability on metre-scale surfaces.

This large scale plasma facility makes use of an ICP torch which is operated at atmospheric pressure. This ICP torch delivers highly collimated and stable energy beam that contains fluorine ions. These ions react with silicon-based substrates to form gases (SiF_4 and SO_2) resulting in material removal. Typically, material removal rate of ~1.5 mm^3/min is achieved. An important feature of the plasma torch is its dedicated nozzle. This nozzle is mounted onto the end of the ICP torch. The nozzle design type and dimensions determine size, shape and plasma velocity of the energy beam.

The processing of metre scale optical surfaces achieved in 2012 was successful both in terms of processing duration and form accuracy. Plasma figuring of a 440mm sized substrate was performed in less than 2.5 hours achieving 30nm RMS form accuracy from an initial 2.5 micrometre PV value. However, Mid Spatial Frequency (MSF) surface errors were measured [6]. These MSF were characterised and correlated to the raster-scanning toolpath parameters and energy beam footprint.

The identified and undesired MSF surface errors needed to be addressed. Consequently, the use of smaller scale energy beams has been suggested [7]. The energy beam footprint achieved in the previous research is shown in Fig. 1. It can be seen that FWHM value is 12mm.

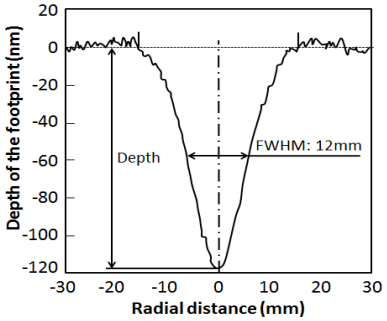

Fig. 1: Cross section of the removal footprint.

The purpose of the work presented in this paper is to advance the plasma figuring of optical surfaces through the creation of a range of energy beams. This objective will be achieved by a fundamental scientific understanding of ICP torches and associated nozzles. Ultimately this research aims at providing highly collimated energy beams characterized by a material removal footprint between 1mm and 5mm FWHM.

Numerical simulations of energy beams are considered essential to investigate and understand the dynamic of the energy beam flow. Works of other research groups have focused on the magneto-hydrodynamics of the plasma within the plasma core.

This paper describes work carried out to create a robust CFD model and to analysis the power dissipation through the torch. The model described in section two enables to predict the behaviour of the energy beam. Therefore the power dissipation analysis is detailed in section three where an attempt is made to derive the energy beam temperature from the correlation between CFD results and experimental measurements. The calculations of different power dissipation items in section four enables establish the energetic balance.

2 CFD simulation

CFD simulations were carried out using the commercial software FLUENT [8]. This CFD package was utilized for the investigation of the aerodynamic behaviour of the RF plasma jet of the energy beam. From a numerical viewpoint the torch modelling is made of two domains. The first domain is a region of intense EM fields where Magnetohydro dynamic calculation is needed. And the second domain is the nozzle-substrate region.

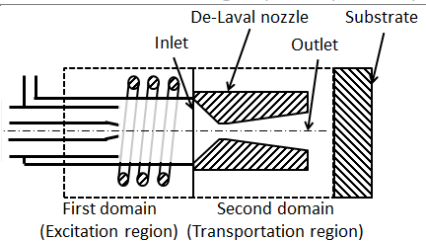

Fig. 2: ICP torch with substrate (numerical domains mentioned)

This CFD investigation focused on the second domain. This domain is characterised by transportation and etching regions. Authors called this media the High Temperature Gas (HTG) throughout this paper.

2.1 Modelling hypothesis

The main modelling assumptions adopted are:

1. HTG flow is axisymmetric, and turbulent;
2. The effect of EM fields is negligible;
3. Viscous dissipation is taken into account;
4. Local Thermal Equilibrium is achieved;
5. The HTG is both thermally expansible and mechanically incompressible.

2.2 Governing equations

We have considered a steady state regime with 2D axisymmetric model based on a HTG that is governed by the Navier-Stokes momentum equation as Eq. (1), conservation of mass as Eq. (2) and (3) and energy transport as Eq. (4).

$$\frac{\partial(\rho v_z)}{\partial z}+\frac{1}{r}\frac{\partial(\rho r v_r)}{\partial r}=0 \quad (1)$$

$$\rho\left[\frac{\partial v_z}{\partial z}v_z+\frac{\partial v_z}{\partial r}v_r\right]=-\frac{\partial p}{\partial z}+\frac{\partial}{\partial z}\left[\mu\left(2\frac{\partial v_z}{\partial z}\right)\right]+\frac{1}{r}\frac{\partial}{\partial r}\left[\mu r\left(\frac{\partial v_r}{\partial z}+\frac{\partial v_z}{\partial r}\right)\right] \quad (2)$$

$$\rho\left[\frac{\partial v_r}{\partial r}v_r+\frac{\partial v_r}{\partial z}v_z\right]=-\frac{\partial p}{\partial r}+\frac{\partial}{\partial r}\left[\mu\left(2\frac{\partial v_r}{\partial r}\right)\right]+\frac{\partial}{\partial z}\left[\mu\left(\frac{\partial v_r}{\partial z}+\frac{\partial v_z}{\partial r}\right)\right]+\frac{2\mu}{r}\left(\frac{\partial v_r}{\partial r}-\frac{v_r}{r}\right) \quad (3)$$

$$\rho\left[\frac{\partial h}{\partial r}v_r+\frac{\partial h}{\partial z}v_z\right]=\frac{\partial}{\partial z}\left(\frac{\lambda}{c_p}\frac{\partial h}{\partial z}\right)+\frac{1}{r}\frac{\partial}{\partial r}\left(r\frac{\lambda}{c_p}\frac{\partial h}{\partial r}\right)+U_P-U_R+U_C \quad (4)$$

where ρ is the gas density, while v_z and v_r stand for the gas velocity in axial and radial directions, respectively; p is the pressure in the nozzle and μ is the viscosity; c_p is the specific heat at a constant pressure, λ is the thermal conductivity and h is static enthalpy.

For ideal incompressible gas, the static enthalpy $h=\sum_j Y_j h_j$, where Y_j is the local mass fraction of species j, and h is the enthalpy of species j. U_P, U_R, U_C are local plasma energy dissipation rate -Joule heating rate-, volumetric radiation heat losses -Radiation losses per unit volume-, and heat of chemical reaction, respectively. In the case of present work, using the

hypothesis mentioned above, U_P and U_C is counted as 0.

2.3 Turbulence characteristics

In the case of the present work, the temperature of the HTG is below 5000 Kelvin [9]. Then the HTG jets' turbulent behaviour is described using the standard k - ε scheme [10]. For computing Reynolds stresses two additional transport equations were solved. Kinetic turbulent energy k and its dissipation rate ε equations are shown in Eq. (5) and Eq. (6).

$$\frac{\partial(\rho k u_i)}{\partial x_i} = \frac{\partial}{\partial x_j}\left[\left(\mu + \frac{\mu_t}{\sigma_k}\right)\frac{\partial k}{\partial x_j}\right] + G_k - \rho\varepsilon \quad (5)$$

$$\frac{\partial(\rho \varepsilon u_i)}{\partial x_i} = \frac{\partial}{\partial x_j}\left[\left(\mu + \frac{\mu_t}{\sigma_\varepsilon}\right)\frac{\partial \varepsilon}{\partial x_j}\right] + C_{1\varepsilon}\frac{\varepsilon G_k}{k} - C_{2\varepsilon}\frac{\rho\varepsilon^2}{k} \quad (6)$$

The quantities of $C_{1\varepsilon}$, $C_{2\varepsilon}$, σ_k and σ_ε are empirical constants [8]. The turbulent viscosity μ_t involves a constant c_μ=0.09 and is derived from k and ε.

2.4 Experimental BC and numerical procedure

In our computational domain, the HTG was a mixture of argon and 0.4% SF_6. This gas mixture is fed into the nozzle through the upper aperture and it flows downward in an axisymmetric manner. From this aperture, the input radial parameters include: flow velocity profile, temperature profile, and pressure. The input temperature of the upper aperture ranges from 1000 to 6500 Kelvin as supported by the measurement of O'Brien [9]. For the sake of simplicity, the temperature of both the Fused Silica substrate and the nozzle are set to 400 Kelvin. The static pressure in the processing chamber is set 101325 Pa (outlet side). Also, the gas temperature of the chamber is 300 Kelvin.

The dimensions of the De-Laval nozzle and the standoff distance between the nozzle and the substrate are displayed below.

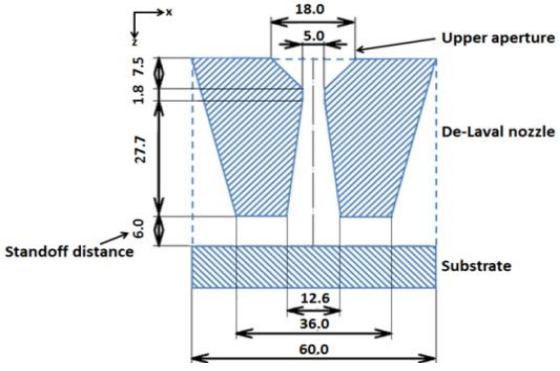

Fig. 3: Nozzle geometry (unit: mm).

3 Estimation of energy dissipation

Through this section, the authors aim to establish the energy balance of the ICP torch and determine the energy absorbed by the coolant.

Fig. 4 illustrates the Plasma Delivery System (PDS) under scrutiny. RF power is provided to the PDS -RF generator, ICP torch and capacitors- to create and maintain the energy beam. This RF power -Forwarded Power (FP) - is consumed by coolants, argon gas flow, and radiation. The global rate of energy balance is:

$$\Delta E_{FP} = \Delta E_{coolant} + \Delta E_{argon} + \Delta E_{radiation} \quad (7)$$

where $\Delta E_{coolant}$ is the rate of energy dissipated by the coolants; ΔE_{argon} is the rate of energy dissipated by the beam; $\Delta E_{radiation}$ is the rate of energy dissipated due to radiations absorbed by surrounding air and the aluminium trumpet.

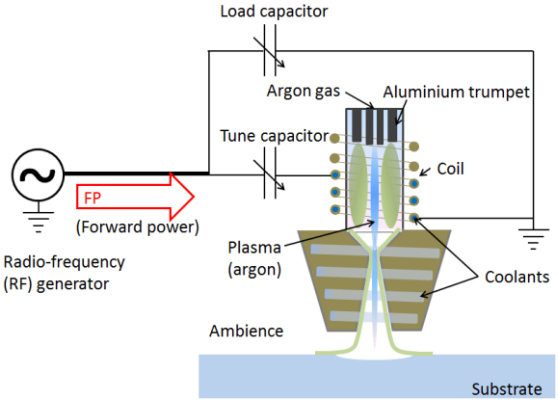

Fig. 4: Schematic of the PDS

This energy rate balance will be investigated through experimental work and calculations. The experiment focuses on temperature of the coolants and is detailed in the next section.

3.1 Energy dissipated by coolants

3.1.1. Experimental set-up

The coolant is used to prevent the oxidation of the coil and the melting of the copper nozzle when the plasma is ignited. The recommended temperature of the coolant is about 20℃. Coolant flows into two main torch components: coil - excitation region- and nozzle -transportation region- (Fig. 2). Fig. 5 illustrates the coolants' distribution.

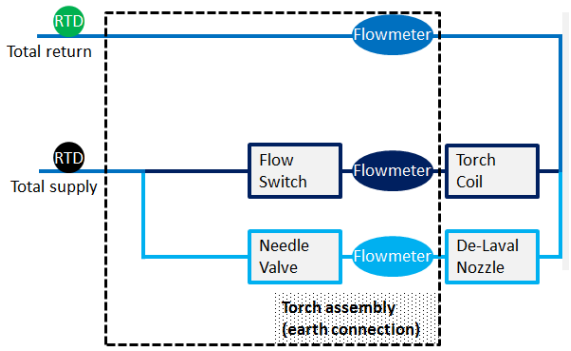

Fig. 5: Schematic of the coolant distribution. (Flow rates were measured using Platon NGX flowmeter)

The supply coolant is divided into two tributaries. The first tributary -navy colour- cooled the torch coil. This flow rate is set to 0.102 GPM (386.6 cm^3/min). The torch nozzle is cooled down by the second tributary of this coolant circuit -cyan colour- . This flow rate is 0.314 GPM (1187 cm^3/min). The chilling coolant is a mixture of water/ethylene glycol (50/50).

3.1.2. Measurements of coolants' temperature

RTDs - OMEGAFILM PT100- were used for these experiments. The RTDs temperature range is from -70℃ to 500℃ with a sensitivity of 0.39% K^{-1}. National Instrument Data acquisition (DAQ) device was used to log the data. All RTDs were calibrated in the icy water and boiling water (zero and hundred degree Celsius). The nonlinearity correction parameter found was 0.385% per 100℃. The measurement uncertainty of these RTDs was down to 0.001 ℃ (0.1% at 0℃).

The RTDs were used to measure the coolants' temperature of both inlet -Total supply- and outlet -Total return-, (see Fig. 5). The Forward Power (FP) was increased from 0 watt to 700 watts through incremental steps of 100 watts every 3 minutes.

Temperature measurements logs are displayed in Fig. 6. The black curve is the inlet coolant temperature, while the green curve is the outlet coolant temperature. The temperature of inlet coolant varies from 18.2 ℃ to 21.1 ℃, which is attributed to the regular cycle of the main chiller.

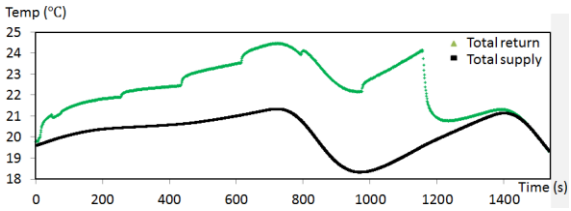

Fig. 6: Temperature logs of the coolants

3.1.3. Temperature difference (TD)

The TD between the inlet and outlet coolant of the torch assembly can be calculated by subtraction (Total return - Total supply). The TD result of each forward power steps is displayed in Fig. 7.

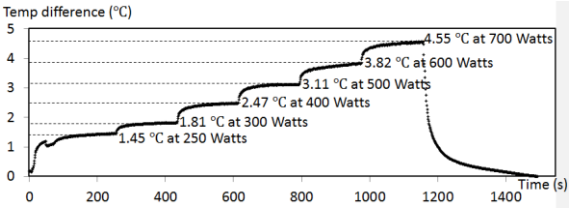

Fig. 7: TD of the coolants through ICP torch

The result above enables to correlate FP and TD values as shown in Fig. 8.

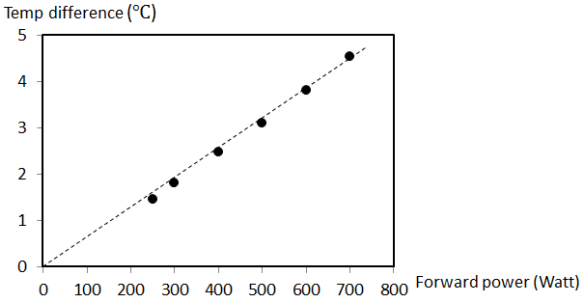

Fig. 8: Correlation between FP and TD values

3.1.4. Energy absorbed by coolants

For a FP value set to 700 watts -steady state condition- the energy absorbed by coolants can be calculated by Eq. (8).

$$\Delta E_{\text{coolant}} = C_c v_c \Delta T \quad (8)$$

where C_c = 3.14 kJ/(kg K) is the specific heat capacity of coolant, (A 50/50 mixture by mass ethylene glycol has a specific heat capacity of three quarters of pure water); v_c = 1055.7035 kg/m^3 x 1.558 l/min = 1.6448 kg/ min is the flow rate; ΔT= 4.55K is the TD value of coolants.

Substituting these values into equation (8), the rate of dissipated energy by the coolants is 23.24 kJ/min (387.35 watts). So the dissipated energy rate -total energy input divided by torch coolants- is 55.34%.

3.2 Energy dissipated by argon gas

3.2.1 Temperature of the HTG in De-Laval nozzle

The average temperature of the HTG in this domain is 912.25 K (Calculates the volume-weighted average on a 3D equivalent location).

Also the calculated distributions for Mach number, temperature in the domain are illustrated in Fig. 9. x-axis is radial distance from the symmetric line, and z-axis is axial distance along the symmetric line. The Mach number reaches the value of 0.56 in the bottle neck of the nozzle. This velocity is still subsonic as expected.

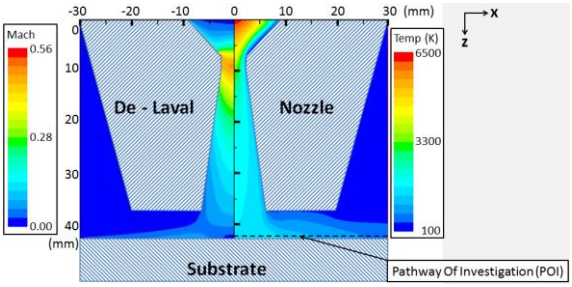

Fig. 9: Calculated distribution of the Mach number (left), temperature of HTG (right).

3.2.2 Derivation of plasma average temperature value

Based on the linear correlation between the FP and TD values, the authors have extrapolated TD value for the nominal processing FP value. Thus the deduced energy loss rate by the coolant for a 1200 watts FP is estimated to 664 watts. Also the energy absorbed by the argon gas can be calculated through Eq. (9)

$$E_{argon} = \int_{T_{room}}^{T} (C_a v_a) dT \quad (9)$$

where v_a=22 l/min (= 0.015576 mol s^{-1}) is the gas flow rate, and C_a (J mol^{-1} K^{-1}) is the specific heat capacity of argon gas given as a function of the temperature of plasma [11], shown as Eq. (10):

$$C_{p\,argon} = 20.8 - 3.2 \times 10^{-5}T + 5.2 \times 10^{-8}T^2 \quad (10)$$

The dissipated energy rate from the argon heating can be integrated using Eq. (10):

$$E_{argon} = v_a(6090.5 + 20.79T - 1.6 \times 10^{-5}T^2 + 1.72 \times 10^{-8}T^3) \quad (11)$$

The fraction of the radiation losses in the total energy balance of ICP torch varied in a wide range: from 8% to 32% [12]. According to Eq. (7), the E_{argon} can be derived. This result is 13% to 37% of the FP. Then the average temperature of plasma was estimated through Eq. (11). Values range from 481.8K to 1370K.

3.2.3 Estimation of energy dissipated from argon gas

The rate of energy dissipated by argon gas is 394.2 watts when the average temperature of argon is 912.25K (CFD result).

3.3 Energy dissipated by radiation(estimated)

The average temperature of the argon gas was calculated as 912.25K through the CFD model. This result is within the range of predicted gas temperatures mentioned in section 3.2.2 (481.8K to 1370K). That previous result was based on the energy dissipation experiment. However, the radiation losses value in [12] is not accurate enough for the overall energy dissipation estimation. The radiative energy dissipated in the present research consists of two parts: excitation region and transportation region (Fig. 10).

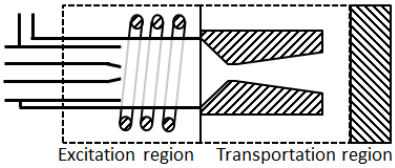

Fig. 10: Radiation regions of the ICP torch

3.3.1 Radiation in excitation region

For the radiation in the excitation region, both Wilbers [13] and Benoy [14] calculated the radiative loss under atmospheric plasma condition as a function of temperature (3000K to 12000K). In the present study, the plasma temperature in the ICP torch is estimated to 10000K [9]. Therefore, the estimated radiative energy dissipated rate in the torch tube ranges from 70 watts to 200 watts, depending on the radius distance from the torch axis.

3.3.2 Radiation in transportation region

The radiative energy dissipated rate in the transportation region can be estimated based on Stefan-Boltzmann law. The radiation energy loss rate can be achieved as 41 watts by Eq. (12).

$$E_{radiation} = e\,\sigma\,A(T^4 - T_C^{\,4}) \quad (12)$$

where e is emissivity (= 0.8 from [12]), σ is Stefan's constant (5.6703x10^{-8} watt/m^2K^4), A is radiating area (1.32 x 10^{-3} m^3 for the axis-symmetric wall of the nozzle), T is average temperature of plasma in the nozzle (912.25K), and T_C is the temperature of nozzle wall (400K).

3.3.3 Total radiation energy

The range of total radiative energy dissipated rate is from 111 watts up to 241 watts, which is 9.25% to 20.1% of FP. This calculation is also within the range of [12].

4 Discussion

In this paper, the percentage of energy dissipated by the coolants is 55.34% (664 watts). This result obtained through experiment and measurements which are qualify as a robust method.

The percentage of energy dissipated by heating the argon gas -calculated through the CFD results- is 32.85% (394.2 watts).

The percentage of energy dissipated by radiation is less robust. The radiations from plasma –excitation and transportation regions calculated in 3.3- is absorbed by surrounding objects: copper coil,

aluminium trumpet, copper nozzle, and air. Some the total radiative energy is clearly dissipated by coil and nozzle. This amount of energy is already counted by the energy dissipated through coolants (section 3.1). Then the authors suggest that the $E_{radiation}$ which is transferred to surrounding air and the aluminium trumpet is still to be defined. To fully quantify radiative energy dissipated in nozzle, coil, substrate and air, further measurements are required.

Fig. 11 illustrates the energy dissipation rates through each component. The rest energy is mainly transferred to the substrate through radiation and convection.

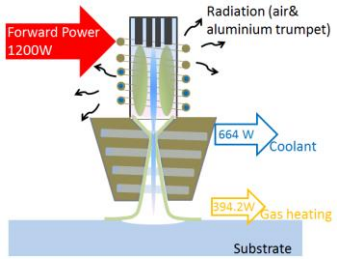

Fig. 11: Sketch of the energy dissipation rate.

5 Conclusion

A CFD model based on the High Temperature Gas (HTG) was developed for a De-Laval nozzle. Experiments were carried out to measure the energy loss of the ICP torch from coolants. The energy for gas heating and loss from radiation were derived. Then the average temperature of plasma was calculated based on these derivations. The HTG average temperature obtained through CFD results is in a good agreement with that derived from the energy dissipation measurements. This research work enables a gross understanding of the plasma figuring in terms of energy dissipation. Further measurements will be carried out for a better estimation of energy balance in the entire system.

6 Acknowledgments

This research work was funded by the Centre for Innovative Manufacturing in Ultra Precision of the Engineering and Physical Sciences Research Council (EPSRC) UK.

7 References

[1] Shore P, Morantz P, Read R, Tonnellier X, Comley P, Jourdain R, Castelli M. Productive Modes for Ultra-Precision Grinding of Freeform Optics. ASPE, Kohala Coast, Hawaii, USA. 26th -27th June, 2014

[2] Shore P, Cunningham C, DeBra D, Evans D, Hough J, Gilmozzi R, Kunzmann H, Morantz P, Tonnellier X. Precision engineering for astronomy and gravity science. CIRP Annals – Manufacturing Technology. 2010; 59: 694–716.

[3] Carr J, Atmospheric Pressure Plasma Processing for Damage - Free Optics and Surfaces. Engineering research Development and Technology. 1999; 3: 31-39.

[4] Jourdain R, Castelli M, Shore P, Sommer P, Proscia D. Reactive atom plasma (RAP) figuring machine for meter class optical surfaces. Production Engineering Research & Development. 2013; 6: 665-673.

[5] Castelli M, Jourdain R, Morantz P, Shore P. Rapid optical surface figuring using reactive atom plasma. Precision Engineering. 2012; 36: 467-476

[6] Jourdain R, Castelli M, Morantz P, Shore P. Plasma Surface Figuring of Large Optical Components. SPIE, Photonics Europe, Belgium, 16th -19th April, 2012

[7] Castelli M. Advances in Optical Surface Figuring by Reactive Atom Plasma (RAP) (PhD thesis), Cranfield University, Cranfield, UK: 2013.

[8] Fluent Inc. 2013 FLUENT Release 15.0, ANSYS Fluent User's Guide. ANSYS Inc

[9] O'Brien W. Characterisation and Material Removal Properties of the RAPTM Process (PhD thesis), Cranfield University, Cranfield, UK: 2011.

[10] Launder, B. E., & Spalding, D. B. (1974). The numerical computation of turbulent flows. Computer methods in applied mechanics and engineering, 3(2), 269-289

[11] Reid, Robert C., John M. Prausnitz, and Bruce E. Poling. "The properties of gases and liquids." (1987).

[12] Gutsol, A. F., J. Larjo, and R. Hernberg. Reverse-flow swirl radio-frequency induction plasmatron. High Temperature 39.2 (2001): 169-179.

[13] Wilbers, A. T. M., J. J. Beulens, and D. C. Schram. "Radiative energy loss in a two-temperature argon plasma." Journal of Quantitative Spectroscopy and Radiative Transfer 46.5 (1991): 385-392.

[14] Benoy, D. A., J. A. M. Van der Mullen, and D. C. Schram. "Radiative energy loss in a non-equilibrium argon plasma." Journal of Physics D: Applied Physics 26.9 (1993): 1408.